

Article

Purifying of Waste Tire Pyrolysis Oil Using an S-ZrO₂/SBA-15-H₂O₂ Catalytic Oxidation Method

Muhammad Nobi Hossain , Myung Kyu Choi, Hoon Chae Park and Hang Seok Choi * 

Department of Environmental Engineering, Yonsei University, Wonju 26493, Korea; mnhossain.8911@gmail.com (M.N.H.); cmg9411@yonsei.ac.kr (M.K.C.); hcpark@yonsei.ac.kr (H.C.P.)

* Correspondence: hs.choi@yonsei.ac.kr; Tel.: +82-33-760-2485; Fax: +82-33-760-2571

Received: 16 March 2020; Accepted: 28 March 2020; Published: 30 March 2020



Abstract: Heavy fuel oils contain a high amount of sulfur. In this work, an extent amount of sulfur content waste tire pyrolysis oil (WTPO) was used as a fuel feedstock. A promising alternative oxidative desulfurization (ODS) method was applied in sulfur removal from WTPO using a S-ZrO₂/SBA-15 solid acid catalyst, hydrogen peroxide (H₂O₂) as an oxidant and acetonitrile as an extracting solvent at varied conditions. The prepared catalyst was characterized by X-ray diffraction (XRD), Bruanuer-Emmet-Teller (BET) method and Fourier transform infrared spectroscopy (FTIR) analysis. The influence of reaction parameters such as reaction time (30–60 min), catalyst loading (0.5–1.5 wt.%), oxidant to oil mole ratio (5–15) at fixed reaction temperature 70 °C on desulfurization of WTPO were investigated. Taguchi method was selected to design the experiment for optimizing the reaction parameters by maximizing the sulfur removal efficiency. The maximum desulfurization efficiency 59.49% was obtained under optimum conditions reaction time (60 min), catalyst loading (1.0 wt.%) and oxidant to sulfur mole ratio (10:1). A catalytic S-ZrO₂/SBA-15 -H₂O₂ oxidation system for oxidative desulfurization of waste tire pyrolysis oil using at mild reaction conditions was developed.

Keywords: optimization; oxidative desulfurization; taguchi method; waste tire oil

1. Introduction

The energy crisis and environmental pollution are the two main problems in the world today due to the increasing human population and rapid industrialization. To meet the fuel energy demand, many initiatives are being taken to find alternative fuel oils due to the depletion of fossil fuels. Fuel oil derived from waste tire pyrolysis is becoming a promising alternative energy source because of its higher heating value and availability [1,2].

A large amount of waste tires is produced every day due to the high demand for personal and commercial transportation. There are several ways to manage the disposal of waste tires, such as landfill deposition and incineration. However, these techniques have limitations due to the availability of land space, possibility of fire at the waste tire storage areas. In addition, some toxic gases and black smog are produced during the incineration of waste tires, which can cause air pollution [3,4].

Waste tires are made of natural rubber, synthetic rubber, fabric, and carbon including other chemicals. Another important component of waste tire is sulfur, which acts as a cross-linking agent. Waste tires have a higher heating value compared to waste biomass. Therefore, waste tires have huge potential for use as an alternative energy source to conventional fuel oils. Usually, waste tire oil is produced using a pyrolysis process. However, the main disadvantage of waste tire pyrolysis oil is its high sulfur content (1–1.4 wt.%) [3–6].

Sulfur is one of the major sources of air pollution, which threatens human health and the surrounding environment. Therefore, it is important to reduce the amount of sulfur in waste tire oil

to make it a green fuel oil and to meet the standard for sulfur content (10–15 ppm) set by the United States Environmental Protection Agency (USEPA) [7–10].

Commercially, hydrodesulfurization (HDS) is used in the oil refinery industry to remove sulfur compounds from liquid fuel oils with a high removal efficiency in the presence of valuable metal catalysts. However, the main drawback of this method is that it needs high temperature (~400 °C) and high pressure (~100 atm), which increase the operational cost. In recent years, the catalytic oxidative desulfurization (ODS) process has drawn attraction due to its milder reaction conditions (low temperature and pressure [11–16]).

The catalytic oxidative desulfurization (ODS) process consists of two steps. In the first step, sulfur containing fuel oil is subjected to catalytic oxidation to produce oxidized sulfur compounds (sulfones/sulfoxides) in the presence of an oxidant. In the second step, the oxidized sulfur compounds are removed from the reaction mixture using an adsorption or liquid/liquid extraction method (Figure 1). Highly polar solvents such as DMF, NMP, DMSO, and acetonitrile are used to extract the sulfur compounds [16–19].

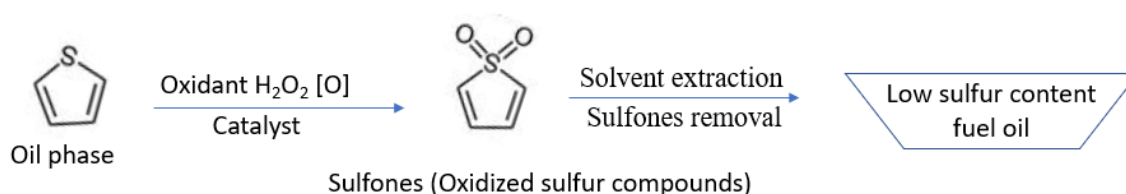


Figure 1. Mechanism of catalytic oxidative desulfurization of fuel oil.

Catalysts play an important and effective role in the ODS process because the catalysts activate the activity of the oxidizing agent. Many catalytic-oxidation systems have been applied in the oxidation of sulfur compounds such as acetic acid/formic acid catalytic/oxidation [20,21], heteropolyacid (HPA) catalytic/oxidation [22,23], ionic liquid catalytic/oxidation [24,25], polyoxometalate catalytic/oxidation, silica and molecular sieve catalytic-oxidation [26,27] and ultrasound assisted/oxidation [28,29]. Among them, transition-metal supported composite catalytic oxidation systems are getting more attention because of their excellent catalytic performance. The acidity of the support such as silica, alumina, silica-alumina and magnesia-alumina and the dispersion of the active sites of the catalyst show high activity on the oxidation of sulfur containing fuel oil.

In the present work, sulfate zirconium oxide ($\text{SO}_4^{2-}/\text{ZrO}_2$) supported by high surface area silica (SBA-15), $\text{S-ZrO}_2/\text{SBA-15}$, superacid catalyst was successfully prepared using a direct wet impregnation method in acidic media and used for desulfurization of waste tire pyrolysis oil (WTPO). It is expected that when an oxidant such as H_2O_2 encounter the acidic sites on sulfated zirconia catalyst, the thermodynamically strong oxidant can be formed, which can oxidize sulfur compounds. The large surface area of $\text{S-ZrO}_2/\text{SBA-15}$ super acid catalyst can enhance the contact between the sulfur compounds and H_2O_2 oxidant. The Taguchi method was selected as the design of the experiment (DOE) to minimize the excess experiments cost and optimize the reaction parameters. The effect of solvent to oil ratio and stirring speed on the sulfur removal of WTPO were studied. In addition, the reusability and stability of the catalyst also was investigated under mild reaction conditions.

2. Results and Discussion

2.1. Catalyst Characterization

2.1.1. X-ray Diffraction

XRD was recorded to observe the mesoporous structure of SBA-15 and crystalline ZrO_2 . The results depicted in Figure 2 show that there are three intense peaks observed at 30° , 50° , and 60° , and two small peaks at 35° and 62° for $\text{SO}_4^{2-}/\text{ZrO}_2$ (S-ZrO_2) calcined at 540°C . These diffraction peaks prove the presence of a bulk ZrO_2 crystalline phase and the absence of other impurities. They also show that

the introduction of sulfate group can stabilize the crystalline phase of ZrO_2 , which is a prerequisite for sulphated zirconia catalytic activity [30]. The XRD pattern of S- ZrO_2 /SBA-15 also shows similar diffraction peaks characteristic of ZrO_2 . The XRD pattern of S- ZrO_2 /SBA-15 also showed one broad intense peak at $20\text{--}30^\circ$, which is characteristic for the hexagonal structure of SBA-15 support [31]. From these findings, it can be concluded that the S- ZrO_2 /SBA-15 solid acid catalyst retains the structure of the SBA-15 support even after it was subjected to the wet impregnation process with ZrO_2 , the introduction of sulfuric acid, and calcination at high temperature.

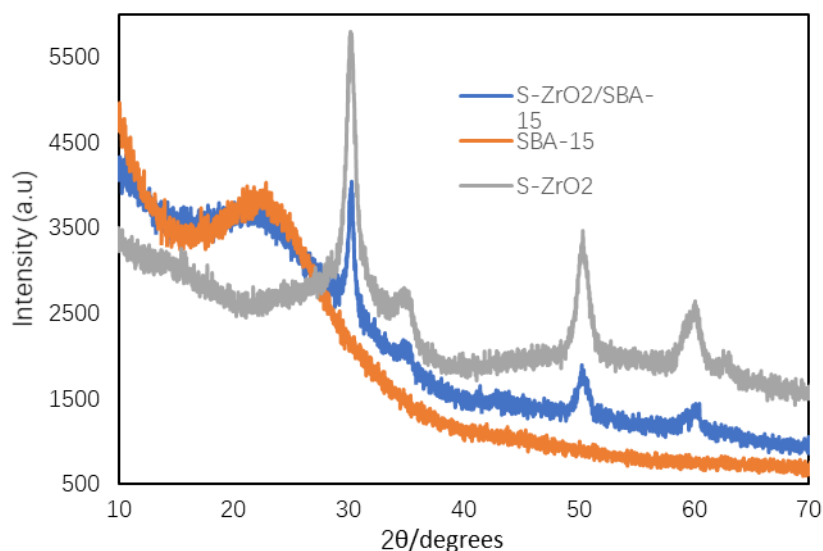


Figure 2. XRD pattern recorded for the S- ZrO_2 /SBA-15 catalyst.

2.1.2. FTIR Spectroscopy

Figure 3 shows the FTIR spectra recorded for the sulfated zirconia SO_4^{2-}/ZrO_2 (S- ZrO_2) and S- ZrO_2 /SBA-15 catalysts. The band observed at $\sim 1400\text{ cm}^{-1}$ is attributed to the covalent S=O bond, which is considered as the characteristic band for SO_4^{2-} for S- ZrO_2 and indicate the strength of its superacidity. This band shifts to $\sim 1530\text{ cm}^{-1}$ in the S- ZrO_2 /SBA-15 catalyst. The band shift can be attributed to the interaction between ZrO_2 and SBA-15 [32]. All the bands observed between 700 and 900 cm^{-1} correspond to the Zr-O-Si bond. This indicates the successful impregnation of zirconia into SBA-15 [33].

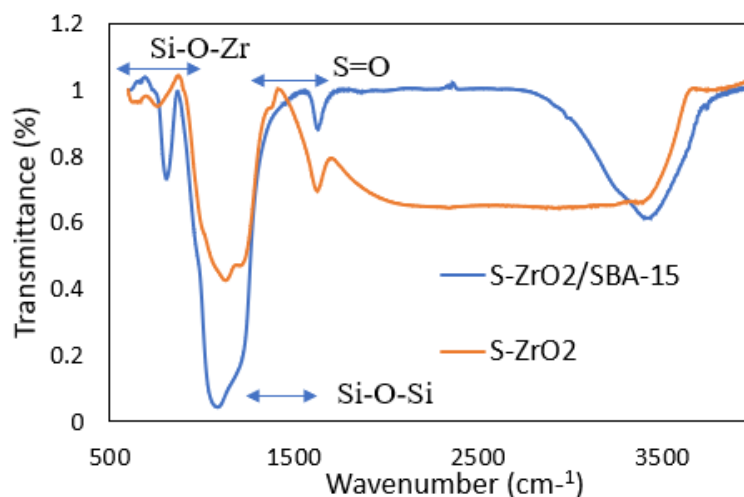


Figure 3. FTIR spectra recorded for S- ZrO_2 and S- ZrO_2 /SBA-15.

2.1.3. Surface Analysis of the Catalysts

The N_2 adsorption-desorption isotherms and pore size distribution of the SBA-15 and S-ZrO₂/SBA-15 catalysts are displayed in Figure 4A, B respectively, and their surface data (surface area, pore volume, and pore size) are presented in Table 1. Figure 4 shows both isotherms were typical IV isotherms with a H1 hysteresis loop, as defined by IUPAC. The hysteresis loop indicates the uniform mesoporous structure of SBA-15 with large dimensions [34,35]. Table 1 shows that the surface area of the SBA-15 support (805.48 m²/g) is decreased to 573.11 m²/g after the incorporation of ZrO₂. Meanwhile, the pore volume and pore diameter also decreased. These results confirm that zirconia was dispersed on the surface of the SBA-15 support.

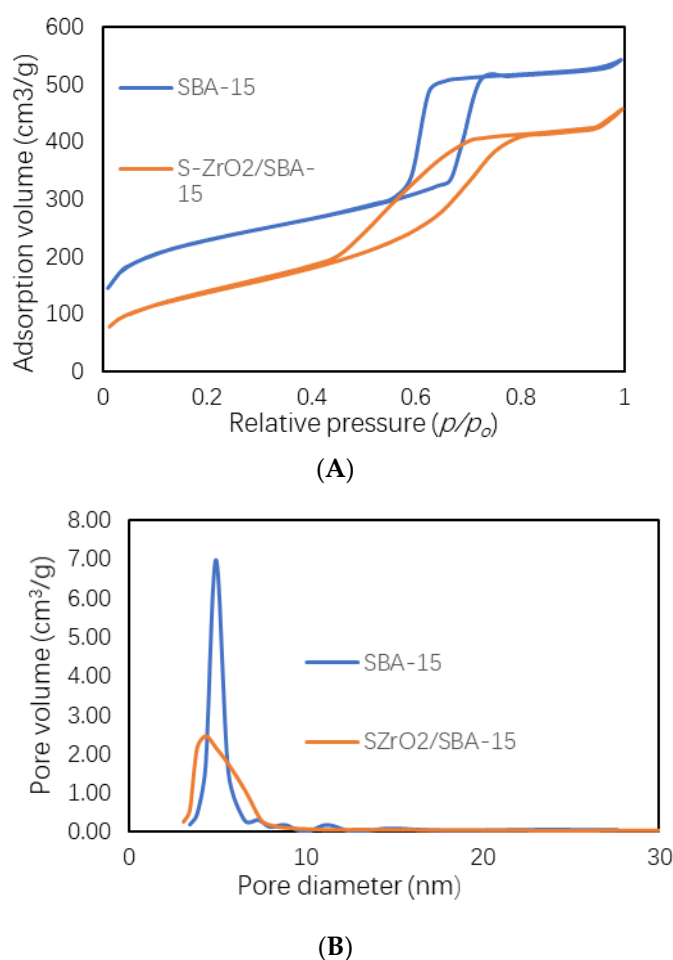


Figure 4. (A) N_2 adsorption-desorption isotherm and (B) Pore size distribution of SBA-15 and S-ZrO₂/SBA-15.

Table 1. The physiochemical properties of SBA-15 and S-ZrO₂/SBA-15.

Catalyst	S_{BET} (m ² /g)	V_p (cm ³ g ⁻¹)	D (nm)
SBA-15	824.07	1.227	4.896
S-ZrO ₂ /SBA-5	496.86	0.690	4.318

2.2. Optimization of the Reaction Parameters

The experimental data was evaluated using the signal to noise ratio (S/N) (Figure 5) according to the Taguchi (L9) orthogonal experimental design method (Table 2). S/N is the ratio between the desired value of the response variable and undesired value of the response variable. The largest S/N

ratio was selected in the optimization of process parameters (reaction time, catalyst and molar ratio of oxidant (H₂O₂) to sulfur) to maximize the sulfur removal efficiency. The S/N ratio was calculated using Equation (1).

$$S/N = 10 \log 1/n (\sum 1/y^2) \quad (1)$$

where n is the number of observations and y is the observed value.

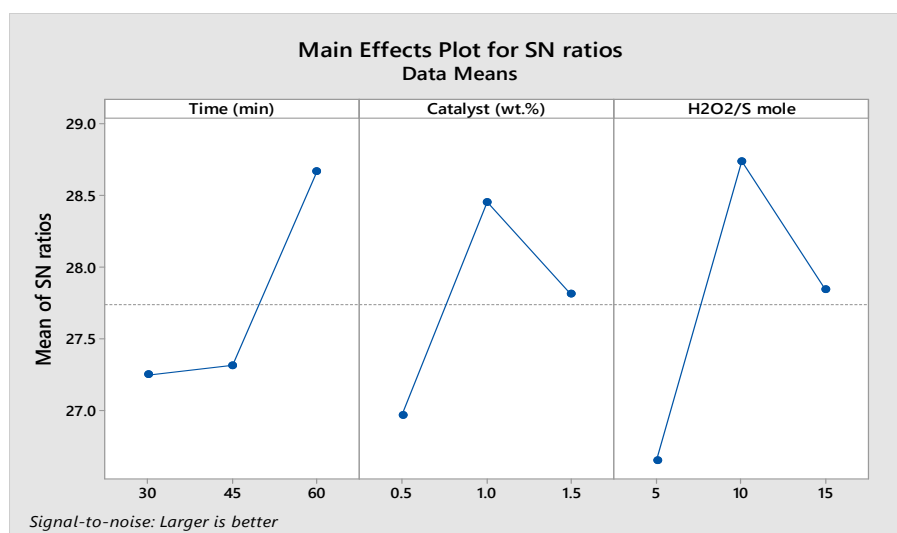


Figure 5. The main effects plot for the S/N ratios.

Table 2. The orthogonal array generated using the Taguchi method to optimize the reaction conditions for upgrading WTPO.

Run	Reaction Parameter			Sulfur Removal Efficiency (%)
	Time (min)	Catalyst Loading (%)	H ₂ O ₂ /S Molar Ratio	
1	30	0.5	5	16.47
2	30	1.0	10	28.94
3	30	1.5	15	25.65
4	45	0.5	10	26.00
5	45	1.0	15	22.59
6	45	1.5	5	21.29
7	60	0.5	15	25.88
8	60	1.0	5	28.35
9	60	1.5	10	27.18

The S/N ratio and main effects plots for the S/N ratio were measured using Minitab 18 software.

The maximum value for the S/N ratio indicates the optimum for the reaction parameter. Figure 5 shows that the maximum sulfur removal efficiency can be achieved using an optimum reaction time of 60 min, 1 wt.% catalyst loading, an oxidant to sulfur (H₂O₂/S) molar ratio of 10:1.

2.3. Statistical Analysis

In the present study, analysis of variance (ANOVA) was performed to identify which parameter in time, catalyst loading, and H₂O₂/S mole ratio significantly affected desulfurization efficiency (Table 3). ANOVA was performed using Minitab 18 statistical software. F-value was used to identify the influence of process parameters [36,37]. Contribution of percentage was also calculated using contribution factor formula. The contribution factor also indicates the significant parameters, but it can be reconfirmed by

F-value [38]. From the Table 3, oxidant to sulfur mole ratio (H_2O_2/S) was the most significant parameter with higher F-value (1.27). The other factors, Time (min) and catalyst loading, followed moderately.

Table 3. The response table for the S/N ratios.

Source	DF	Adj SS	Adj MS	F-Value	Percentage (%)	Rank
Time (min)	2	26.83	13.41	0.80	29.2	2
Catalyst loading (wt.%)	2	22.16	11.08	0.66	24.4	3
H_2O_2/S mole ratio	2	42.72	21.36	1.27	46.58	1
Errors	2	33.54	16.74	-	-	-
Total	8	125.25	-	-	-	-

DF = degrees of freedom, Adj SS = adjusted sum of square, Adj MS = adjusted means of square, F = Probability distribution

2.4. The Effect of the Extracting Solvent to Oil Ratio on the Desulfurization Reaction

The concentration of sulfur decreased upon increasing the solvent to oil ratio (v/v). The amount of sulfur initially decreased rapidly and then slowed down gradually. When the amount of solvent was increased, the miscibility between solvent and oxidized sulfur compounds (sulfoxides/sulfones) increased, which increased the rate of desulfurization. Figure 6 shows that the highest desulfurization efficiency was achieved at a solvent to oil ratio of 4. Therefore, a solvent to oil ratio of 4 was selected in our further experiments.

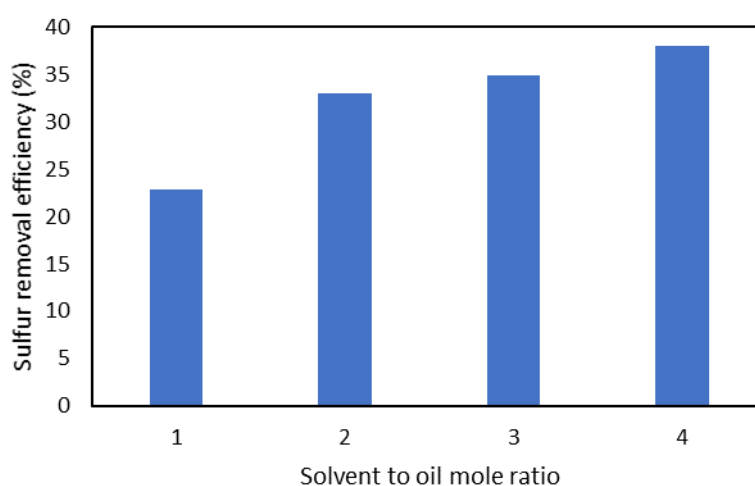


Figure 6. The effect of the molar ratio of solvent to oil (v/v) on the desulfurization of WTPO.

2.5. The Effect of Stirring Speed on the Desulfurization Reaction

The effect of stirring rate on desulfurization of WTPO was also investigated because the sulfur removal efficiency is highly dependent on the contact between the raw oil and catalyst. The sulfur removal efficiency may be high due to efficient mixing between the oil and catalyst [39,40]. Figure 7 shows that the desulfurization efficiency increased upon increasing the stirring rate. When the stirring rate was increased up to 400 rpm, the reaction mixture (oil, catalyst, and oxidant) was mixed uniformly and the sulfur removal efficiency was increased. There was a slight change in the desulfurization efficiency when stirring speed was further increased to 450 rpm. Therefore, 400 rpm was selected as the optimum stirring rate for our further experiments.

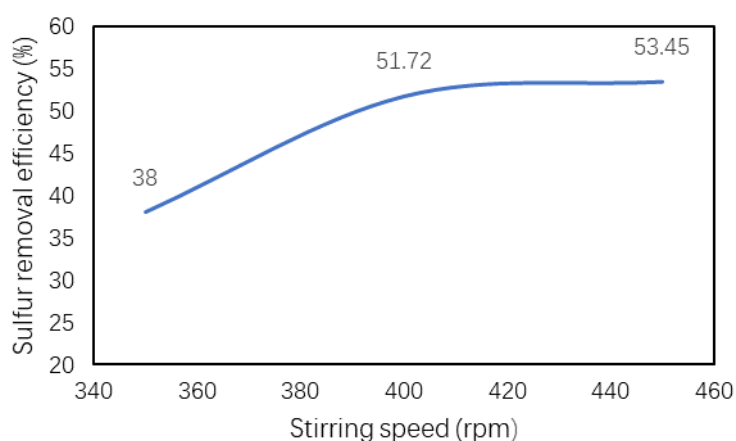


Figure 7. The effect of the stirring rate (rpm) on the desulfurization of waste tire pyrolysis oil (WTPO).

2.6. A Comparison of Different Catalysts on the Desulfurization of Waste Tire Oil

The effects of different types of catalysts on the desulfurization of waste tire oil via oxidative desulfurization were studied. The catalytic activity of ZrO_2 , S-ZrO_2 , and $\text{S-ZrO}_2/\text{SBA-15}$ were evaluated under the optimum conditions. Figure 8 shows that the catalytic performances of the different catalysts were in the following order: $\text{S-ZrO}_2/\text{SBA-15} > \text{SO}_4^{2-}/\text{ZrO}_2 > \text{ZrO}_2$. The sulfur removal efficiency of $\text{S-ZrO}_2/\text{SBA-15}$ was high when compared to the other bulk catalysts (ZrO_2 and $\text{SO}_4^{2-}/\text{ZrO}_2$).

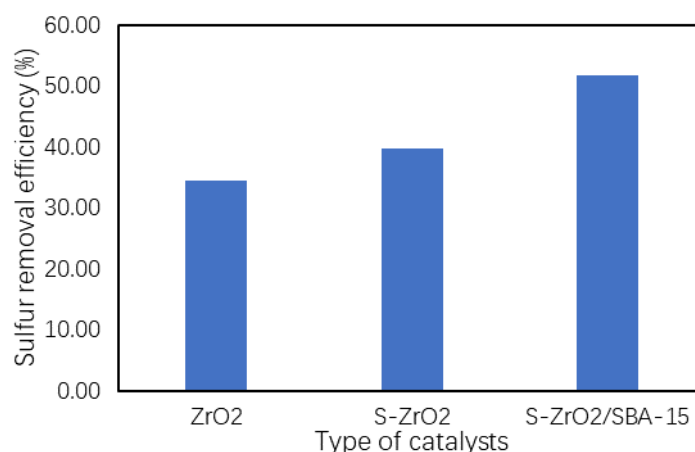
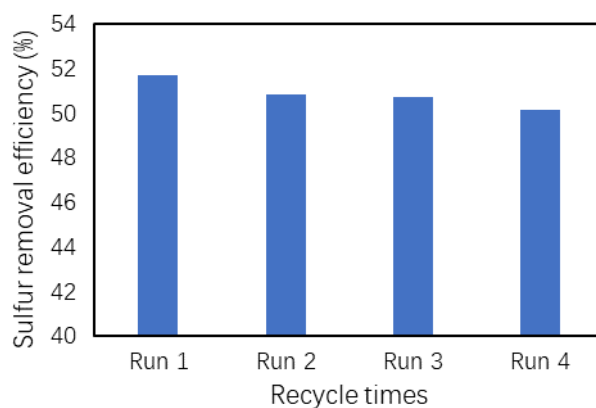


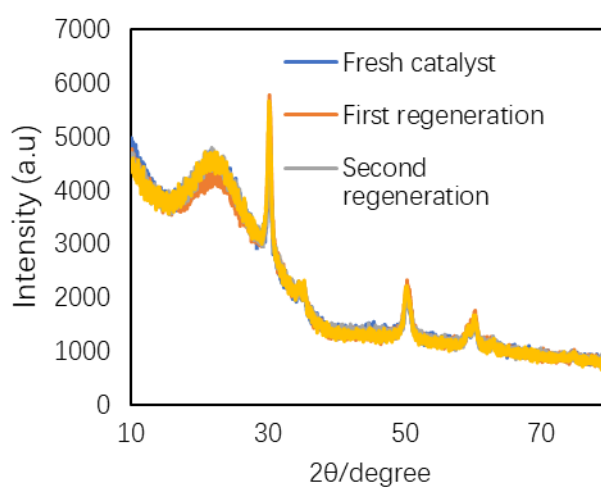
Figure 8. The effect of different type of catalyst on the desulfurization of waste tire oil.

2.7. Reusability of the Catalyst

The reusability of synthesized heterogeneous acid catalyst was studied to investigate its stability. After each catalytic run, the catalyst was separated using filtration, washed with acetonitrile, dried at $80\text{ }^\circ\text{C}$ for 1–2 h, and regenerated upon calcination at $540\text{ }^\circ\text{C}$ for 6 h. The regenerated catalyst was used again in the next run under the same reaction conditions. The results obtained for the ODS reactions after recycling the catalyst several times are presented in Figure 9. They show that the sulfur removal efficiency was comparable to the fresh catalyst after three cycles. This was attributed to the high stability of the $\text{S-ZrO}_2/\text{SBA-15}$ catalyst during the oxidative desulfurization process [41]. To observe the structural stability of the catalyst after several cycles, the XRD patterns of regenerated catalysts were recorded. The results are depicted in Figure 9.



(A)



(B)

Figure 9. (A) Recycling the S-ZrO₂/SBA-15 catalyst in the ODS of WTPO. (B) A comparison of the XRD patterns recorded for the S-ZrO₂/SBA-15 catalyst after three cycles.

2.8. The Effect of the Number of Extraction Steps on the Desulfurization Reaction

The number of extraction steps can play a significant role in the removal of the oxidized sulfur compounds during the extraction of waste tire oil. It is expected that the desulfurization efficiency will be increased upon increasing the number of extraction steps in order to improve the extraction efficiency of the oxidized sulfur compounds [42]. In this study, the extraction of the oxidized sulfur compounds was investigated using acetonitrile as the extracting solvent. Figure 10 shows that the sulfur removal efficiency was increased upon increasing the number of extraction steps from 1 to 3. Therefore, multiple extraction steps were very effective to reduce the sulfur content in WTPO.

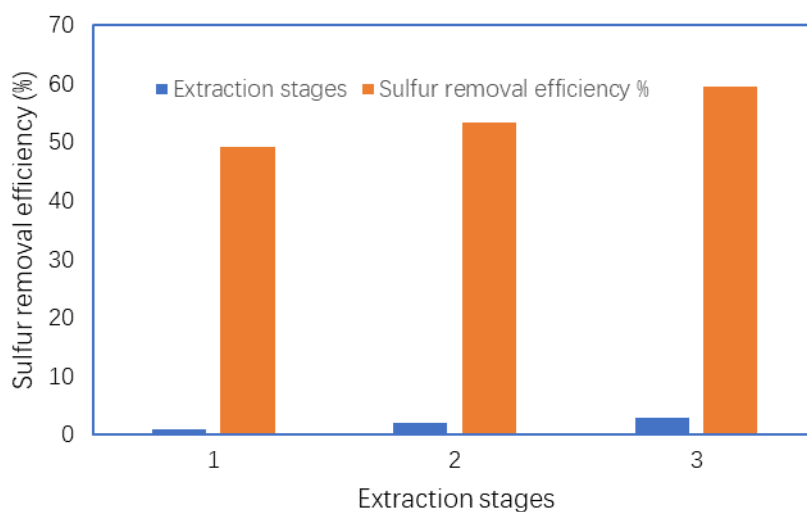


Figure 10. The effect of multiple extraction steps on the desulfurization reaction.

2.9. FTIR Analysis

The FTIR spectra of WTPO before and after the desulfurization process are presented in Figure 11. The peaks observed in the region between 1035 to 1328 cm^{-1} correspond to the sulfoxide and sulfone derivatives, respectively [39,43,44]. Figure 11 shows that after the desulfurization process the peaks corresponding to the sulfur compounds were decreased, which confirms that they were partially removed after oxidation followed by extraction with acetonitrile.

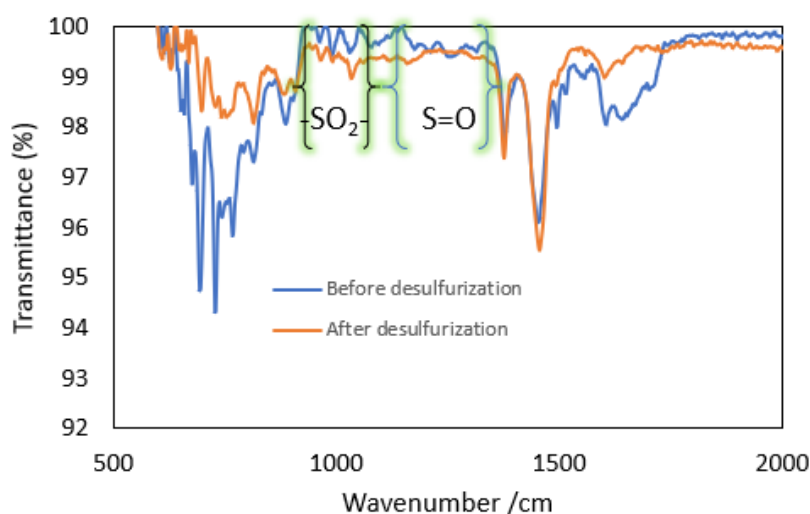


Figure 11. FTIR spectra of waste tire pyrolysis oil before and after oxidation-extraction.

3. Materials and Methods

3.1. Collection of Crude WTPO

WTPO was produced and collected from the CECP laboratory, Department of Environmental Engineering, Yonsei University, Korea. Passenger side car tires were used as raw materials and were obtained from the waste tire disposal facility in Busan, Korea. The pyrolysis reaction was carried out in a conical spouted bed reactor. The characteristics of crude WTPO are presented in Table 4.

Table 4. The characteristics of crude WTPO.

Properties	Value (%)	Method
Elemental analysis		
Carbon	85.599	ASTM D3176
Hydrogen	8.973	
Nitrogen	0.661	
Oxygen	4.767	
Total sulfur	1.16	
Proximate analysis		
Moisture	19.76	ASTM E 1131
Ash	0.78	
Volatile	77.23	
Fixed carbon	2.22	
Heating value	43.8 MJ/Kg	

3.2. Materials and Feedstock

Zirconium hydroxide and Pluronic P123 were obtained from Sigma-Aldrich Co., (St. Louis, MO, USA). Hydrochloric acid (HCl) and sulfuric acid were purchased from Dae-Jung Chemical & Metals Co., Ltd., Gyeonggi-do, Korea. Tetraethyl orthosilicate (C₈H₂₀O₄Si, 98%) was purchased from ACROS Organics Co., (Morris, NJ, USA). These chemicals were reagent grade. Hydrogen peroxide and acetonitrile were purchased from Daejung Chemical & Metals Co., Ltd., Gyeonggi-do, Korea.

3.3. Catalyst Preparation

Sulfated zirconium oxide supported by SBA-15 (S-ZrO₂/SBA-15) was synthesized using a direct wet impregnation method using SBA-15 and the desired amount of zirconium hydroxide, according to the following method with some modification [31]. Sulphated Zr (OH)₄ and Zr (OH)₄/SBA-15 were filtered, dried at 80 °C for 2 h, and calcined at 540 °C for 6 h to give SO₄²⁻/ZrO₂ (S-ZrO₂) and S-ZrO₂/SBA-15.

3.4. Catalytic ODS of WTPO

3.4.1. ODS of WTPO

All ODS reactions were carried out in a 350 mL stainless steel batch reactor equipped with a magnetic stirrer and condenser (Joyoung al-tex Co. Ltd. Model TPS20-G2, Daejon, Korea) Before running the reaction, nitrogen gas was purged due to provide an inert atmosphere inside the reaction vessel and reaction medium. In each run, 50 mL of WTPO was charged into the reaction vessel. Subsequently, a certain amount of catalyst and oxidant were added to the reaction vessel. The reaction mixture was heated to the target temperature (70 °C) and then was stirred at 400 rpm under atmospheric pressure.

3.4.2. Extraction of Desulfurized WTPO

After completing the reaction, the catalyst was recovered via filtration and then the extracting solvent was used to extract the oxidized sulfur compounds. Acetonitrile was used as the extracting solvent at a solvent /oil ratio of 2:1 in the decanter. Then, the decanter was shaken for 30 min and kept overnight for phase separation (oil-solvent phase). Two layers were formed (solvent and oil layer). Finally, the extracted oil phase was collected, and the sulfur content determined by elemental analysis (ASTM D3176). The sulfur removal efficiency was calculated using Equation (2) [7,17]

$$\text{Sulfur removal efficiency (\%)} = [1 - S_0/S_t] \quad (2)$$

where S_0 and S_t represent the initial and final concentration of sulfur after the ODS reaction, respectively.

3.5. Experimental Design for the ODS of WTPO

The Taguchi method was selected to design the experiments used to optimize the sulfur removal efficiency of the ODS reaction of WTPO. The Taguchi method is a very fruitful DOE approach, which not only determines the impact of the reaction parameters, but also reduce the production cost and time [32,45]. The effect of the oxidant, catalyst loading, and reaction time on the desulfurization reaction were investigated. The experimental range and reaction parameters are presented in Table 5.

Table 5. The design of the optimization experiments.

Reaction Parameter	Number of Levels	Value
Time (min)	3	30 45 60
Catalyst loading (wt.%)	3	0.5 1.0 1.5
Molar ratio of oxidant (H_2O_2) to sulfur	3	5 10 15

Using statistical software (Minitab 18), an orthogonal array was formed based on the Taguchi method to generate the number of reactions to be carried out to investigate the effect of the reaction parameters with different levels.

4. Conclusions

Solid superacid catalyst S-ZrO₂/SBA-15 has been successfully prepared using a direct wet impregnation method. The analytical results obtained from XRD, BET, and FTIR confirm the structure and properties of the as-synthesized catalyst. S-ZrO₂/SBA-15 was evaluated in the removal of sulfur compounds from waste tire oil by developing a moderate oxidation desulfurization process. The experiment was designed using the Taguchi method to save additional experimental cost and all reactions were run to maximize the sulfur removal efficiency using H₂O₂ as the oxidant, S-ZrO₂/SBA-15 as the catalyst, and acetonitrile as the extracting solvent. The signal to noise ratio was selected to optimize the reaction parameters. The maximum desulfurization efficiency (59.13%) was obtained under the optimum reaction conditions (reaction time, 60 min; catalyst loading, 1.0 wt.%; H₂O₂ molar ratio of H₂O₂, 10:1; and extracting solvent acetonitrile to oil ratio, 4:1 (*v/v*) at fixed reaction temperature 70 °C). Multi-step extraction was effective in reducing the amount of sulfur in the fuel oil feedstock. The catalyst was successfully recycled three times, which indicates its high catalytic stability. The stability of catalyst was further confirmed using XRD after its reuse. The results indicate that S-ZrO₂/SBA-15-H₂O₂ catalytic oxidation system has potential in the purifying process of WTPO by reducing the sulfur content under mild reaction conditions.

Author Contributions: Conceptualization, H.S.C. & M.N.H.; Methodology, M.N.H.; Software, M.N.H.; Formal Analysis, M.N.H.; Data curation, M.N.H. & M.K.C.; Writing-Original draft preparation, M.N.H.; Writing-Review & Editing, H.S.C.; Visualization, M.K.C. & H.C.P.; Supervision, H.S.C.; Funding acquisition, H.S.C. All authors have read and agreed to the published version of the manuscript.

Funding: This work was supported by the National Research Foundation of Korea (NRF) grant funded by the Ministry of Science, ICT, and Future Planning (MSIP) of Korea (NRF-2017R1A2B4009340). This work was supported by the Korea Institute of Energy Technology Evaluation and Planning (KETEP) and the Ministry of Trade, Industry & Energy (MOTIE) of the Republic of Korea (No. 20184030202240).

Acknowledgments: We thank Ministry of Science, ICT, and Future Planning (MSIP) of Korea and the Korea Institute of Energy Technology Evaluation and Planning (KETEP) of the Republic of Korea for their financial support.

Conflicts of Interest: The authors declare that they have no known competing financial interests or personal relationships that could have appeared to influence the work reported in this paper.

References

1. Mia, M.; Islam, A.; Rubel, R.I.; Islam, M.R. Fractional Distillation & Characterization of Tire Derived Pyrolysis Oil. *Int. J. Eng. Technol. IJET* **2017**, *3*, 1–10. [[CrossRef](#)]
2. Al-Marshed, A.; Hart, A.; Leeke, G.; Greaves, M.; Wood, J. Optimization of Heavy Oil Upgrading Using Dispersed Nanoparticulate Iron Oxide as a Catalyst. *Energy Fuels* **2015**, *29*, 6306–6316. [[CrossRef](#)]
3. Trongkaew, P.; Utistham, T.; Reubroycharoen, P.; Hinchiranan, N. Photocatalytic Desulfurization of Waste Tire Pyrolysis Oil. *Energies* **2011**, *4*, 1880–1896. [[CrossRef](#)]
4. Ahmad, S.; Ahmad, M.I.; Naeem, K.; Humayun, M.; Faheem, F. Oxidative desulfurization of tire pyrolysis oil. *Chem. Ind. Chem. Eng. Q.* **2016**, *22*, 249–254. [[CrossRef](#)]
5. Chang, Y.-M. On pyrolysis of waste tire: Degradation rate and product yields. *Resour. Conserv. Recycl.* **1996**, *17*, 125–139. [[CrossRef](#)]
6. Cao, Q.; Jin, L.; Bao, W.; Lv, Y. Investigations into the characteristics of oils produced from co-pyrolysis of biomass and tire. *Fuel Process. Technol.* **2009**, *90*, 337–342. [[CrossRef](#)]
7. Rezvani, M.A.; Shaterian, M.; Aghbolagh, Z.S.; Babaei, R. Oxidative desulfurization of gasoline catalyzed by IMID@PMA@CS nanocomposite as a high-performance amphiphilic nanocatalyst. *Environ. Prog. Sustain. Energy* **2018**, *37*, 1891–1900. [[CrossRef](#)]
8. Ribeiro, S.O.; Julião, D.; Cunha-Silva, L.; Domingues, V.F.; Valença, R.; Ribeiro, J.C.; de Castro, B.; Balula, S.S. Catalytic oxidative/extractive desulfurization of model and untreated diesel using hybrid based zinc-substituted polyoxometalates. *Fuel* **2016**, *166*, 268–275. [[CrossRef](#)]
9. González-García, O.; Cedeño-Caero, L. V-Mo based catalysts for oxidative desulfurization of diesel fuel. *Catal. Today* **2009**, *148*, 42–48. [[CrossRef](#)]
10. Hossain, M.N.; Park, H.C.; Choi, H.S. A Comprehensive Review on Catalytic Oxidative Desulfurization of Liquid Fuel Oil. *Catalysts* **2019**, *9*, 229. [[CrossRef](#)]
11. Ismagilov, Z.; Yashnik, S.; Kerzhentsev, M.; Parmon, V.; Bourane, A.; Al-Shahrani, F.M.; Hajji, A.A.; Koseoglu, O. Oxidative Desulfurization of Hydrocarbon Fuels. *Catal. Rev.* **2011**, *53*, 199–255. [[CrossRef](#)]
12. Choi, A.E.; Roces, S.; Dugos, N.P.; Wan, M.-W. Oxidation by H₂O₂ of bezothiophene and dibenzothiophene over different polyoxometalate catalysts in the frame of ultrasound and mixing assisted oxidative desulfurization. *Fuel* **2016**, *180*, 127–136. [[CrossRef](#)]
13. Jiang, B.; Yang, H.; Zhang, L.; Zhang, R.; Sun, Y.; Huang, Y. Efficient oxidative desulfurization of diesel fuel using amide-based ionic liquids. *Chem. Eng. J.* **2016**, *283*, 89–96. [[CrossRef](#)]
14. Rezvani, M.A.; Khandan, S.; Sabahi, N. Oxidative Desulfurization of Gas Oil Catalyzed by (TBA)4PW11Fe@PbO as an Efficient and Recoverable Heterogeneous Phase-Transfer Nanocatalyst. *Energy Fuels* **2017**, *31*, 5472–5481. [[CrossRef](#)]
15. Dai, Y.; Qi, Y.; Zhao, D.; Zhang, H. An oxidative desulfurization method using ultrasound/Fenton's reagent for obtaining low and/or ultra-low sulfur diesel fuel. *Fuel Process. Technol.* **2008**, *89*, 927–932. [[CrossRef](#)]
16. Abdelrahman, A.A.; Betiha, M.; Rabie, A.M.; Ahmed, H.S.; El-Shahat, M. Removal of refractory Organo sulfur compounds using an efficient and recyclable {Mo132} nanoball supported graphene oxide. *J. Mol. Liq.* **2018**, *252*, 121–132. [[CrossRef](#)]
17. Jalali, M.R.; Sobati, M.A. Intensification of oxidative desulfurization of gas oil by ultrasound irradiation: Optimization using Box–Behnken design (BBD). *Appl. Therm. Eng.* **2017**, *111*, 1158–1170. [[CrossRef](#)]
18. Abu Bakar, W.; Ali, R.; Kadir, A.A.A.; Mokhtar, W.N.A.W. Effect of transition metal oxides catalysts on oxidative desulfurization of model diesel. *Fuel Process. Technol.* **2012**, *101*, 78–84. [[CrossRef](#)]
19. Kadijani, J.A.; Narimani, E.; Kadijani, H.A. Oxidative desulfurization of organic sulfur compounds in the presence of molybdenum complex and acetone as catalysts. *Pet. Coal* **2014**, *56*, 116–123.
20. Mamaghani, A.H.; Fatemi, S.; Asgari, M. Investigation of Influential Parameters in Deep Oxidative Desulfurization of Dibenzothiophene with Hydrogen Peroxide and Formic Acid. *Int. J. Chem. Eng.* **2013**, *2013*, 951045. [[CrossRef](#)]
21. Otsuki, S.; Nonaka, T.; Takashima, N.; Qian, W.; Ishihara, A.; Imai, T.; Kabe, T. Oxidative Desulfurization of Light Gas Oil and Vacuum Gas Oil by Oxidation and Solvent Extraction. *Energy Fuels* **2000**, *14*, 1232–1239. [[CrossRef](#)]

22. Li, S.W.; Gao, R.; Zhang, W.; Zhang, Y.; Zhao, J. Heteropolyacids supported on macroporous materials POM@MOF-199@LZSM-5: Highly catalytic performance in oxidative desulfurization of fuel oil with oxygen. *Fuel* **2018**, *221*, 1–11. [[CrossRef](#)]
23. Rafiee, E.; Nobakht, N. Keggin type heteropolyacid, encapsulated in metal-organic framework: A heterogeneous and recyclable nanocatalyst for selective oxidation of sulfides and deep desulfurization of model fuels. *J. Mol. Catal. A Chem.* **2015**, *398*, 17–25. [[CrossRef](#)]
24. Jiang, W.; Zhua, W.; Chang, Y.; Chao, Y.; Yin, S.; Liu, H.; Zhu, F.; Li, H. Ionic liquid extraction and catalytic oxidative desulfurization of fuels using dialkylpiperidinium tetrachloroferrates catalyst. *Chem. Eng. J.* **2014**, *250*, 48–54. [[CrossRef](#)]
25. Zhang, L.; Wang, J.; Sun, Y.; Jiang, B.; Yang, H. Deep oxidative desulfurization of fuels by superbase-derived Lewis acidic ionic liquids. *Chem. Eng. J.* **2017**, *328*, 445–453. [[CrossRef](#)]
26. Shiraiishi, Y.; Naito, T.; Hirai, T. Vanadosilicate molecular sieve as a catalyst for oxidative desulfurization of light oil. *Ind. Eng. Chem. Res.* **2003**, *42*, 6034–6039. [[CrossRef](#)]
27. Zhao, N.; Li, S.; Wang, J.; Zhang, R.; Gao, R.; Zhao, J.; Wang, J. Synthesis and application of different phthalocyanine molecular sieve catalyst for oxidative desulfurization. *J. Solid-State Chem.* **2015**, *225*, 347–353. [[CrossRef](#)]
28. Gildo, P.J.; Dugos, N.; Wan, S.R.M. Optimized ultrasound-assisted oxidative desulfurization process of simulated fuels over activated carbon-supported phosphotungstic acid. *MATEC Web Conf.* **2018**, *156*, 03045. [[CrossRef](#)]
29. Margeta, D.; Sertić-Bionda, K.; Foglar, L. Ultrasound assisted oxidative desulfurization of model diesel fuel. *Appl. Acoust.* **2016**, *103*, 202–206. [[CrossRef](#)]
30. Xia, Q.-H.; Hidajat, K.; Kawi, S. Synthesis of SO₄²⁻/ZrO₂/MCM-41 as a new superacid catalyst. *Chem. Commun.* **2000**, 2229–2230. [[CrossRef](#)]
31. Hossain, M.N.; Bhuyan, S.; Alam, A.H.M.A.; Seo, Y.C.; Bhuyan, S.U.S. Biodiesel from Hydrolyzed Waste Cooking Oil Using a S-ZrO₂/SBA-15 Super Acid Catalyst under Sub-Critical Conditions. *Energies* **2018**, *11*, 299. [[CrossRef](#)]
32. Zolfaghari, G.; Esmaili-Sari, A.; Anbia, M.; Younesi, H.; Amirmahmoodi, S.; Ghafarinazari, A. Taguchi optimization approach for Pb(II) and Hg(II) removal from aqueous solutions using modified mesoporous carbon. *J. Hazard. Mater.* **2011**, *192*, 1046–1055. [[CrossRef](#)] [[PubMed](#)]
33. Erdem, S.; Erdem, B.; Oksuzoglu, R.M.; Çitak, A. Effect of calcination temperature on the structural and magnetic properties of Ni/SBA-15 nanocomposite. *J. Porous Mater.* **2015**, *22*, 689–698. [[CrossRef](#)]
34. Yu, J.; Shen, A.; Cao, Y.; Lu, G. Preparation of Pd-Diimine@SBA-15 and Its Catalytic Performance for the Suzuki Coupling Reaction. *Catalysts* **2016**, *6*, 181. [[CrossRef](#)]
35. Sanjini, N.S.; Velmathi, S. Iron impregnated SBA-15, a mild and efficient catalyst for the catalytic hydride transfer reduction of aromatic nitro compounds. *RSC Adv.* **2014**, *4*, 15381. [[CrossRef](#)]
36. Tseng, K.-H.; Shiao, Y.-F.; Chang, R.-F.; Yeh, Y.-T. Optimization of Microwave-Based Heating of Cellulosic Biomass Using Taguchi Method. *Materials* **2013**, *6*, 3404–3419. [[CrossRef](#)]
37. Banisharif, F.; Dehghani, M.; Campos-Martin, J.M. Oxidative Desulfurization of Diesel Using Vanadium-Substituted Dawson-Type Emulsion Catalysts. *Energy Fuels* **2017**, *31*, 5419–5427. [[CrossRef](#)]
38. Satya, S.; Kolakoti, A.; Rao, R. Optimization of palm methyl ester and its effect on fatty acid compositions and cetane number. *Math. Models Eng.* **2019**, *5*, 25–34. [[CrossRef](#)]
39. Tang, X.-D.; Hu, T.; Li, J.-J.; Wang, F.; Qing, D.-Y. Deep desulfurization of condensate gasoline by electrochemical oxidation and solvent extraction. *RSC Adv.* **2015**, *5*, 53455–53461. [[CrossRef](#)]
40. De Luna, M.D.G.; Wan, M.-W.; Golosinda, L.R.; Futralan, C.M.; Lu, M.-C. Kinetics of Mixing-Assisted Oxidative Desulfurization of Dibenzothiophene in Toluene Using a Phosphotungstic Acid/Hydrogen Peroxide System: Effects of Operating Conditions. *Energy Fuels* **2017**, *31*, 9923–9929. [[CrossRef](#)]
41. Rezvani, M.A.; Shaterian, M.; Akbarzadeh, F.; Khandan, S. Deep oxidative desulfurization of gasoline induced by PMoCu@MgCu₂O₄-PVA composite as a high-performance heterogeneous nanocatalyst. *Chem. Eng. J.* **2018**, *333*, 537–544. [[CrossRef](#)]
42. Sobati, M.A.; Dehkordi, A.M.; Shahrokhi, M. Extraction of Oxidized Sulfur-Containing Compounds of Non-Hydrotreated Gas Oil. *Chem. Eng. Technol.* **2010**, *33*, 1515–1524. [[CrossRef](#)]
43. Shakirullah, M.; Ahmad, W.; Ahmad, I.; Ishaq, M. Oxidative desulphurization study of gasoline and kerosene. *Fuel Process. Technol.* **2010**, *91*, 1736–1741. [[CrossRef](#)]

44. Shen, Y.; Sun, T.; Liu, X.; Jia, J. Rapid desulfurization of CWS via ultrasonic enhanced metal boron hydrides reduction under ambient conditions. *RSC Adv.* **2012**, *2*, 4189–4197. [[CrossRef](#)]
45. Soltanieh, M.; Heidarinasab, A.; Ardjmand, M.; Ahmadpanahi, H.; Bahmani, M. Impact of support on the catalytic behavior of Mo/ γ -Al₂O₃ and Mo/MgO catalysts on the desulfurization reaction. *Appl. Catal. A Gen.* **2016**, *516*, 41–50. [[CrossRef](#)]



© 2020 by the authors. Licensee MDPI, Basel, Switzerland. This article is an open access article distributed under the terms and conditions of the Creative Commons Attribution (CC BY) license (<http://creativecommons.org/licenses/by/4.0/>).